Designer co-beta-peptide copolymer selectively targets resistant and biofilm Gram-negative bacteria

Zhangyong Si[1#], Jianguo Li[2,3#], Lin Ruan[1], Sheethal Reghu[1], Ooi Ying Jie[1], Peng Li[4], Yabin Zhu[5], Paula T. Hammond[6,7], Chandra S.Verma[2,8,9], Guillermo C. Bazan[10,11]*, Kevin Pethe[9,12]*, Mary B. Chan-Park[1,12,13]*

[1]School of Chemical and Biomedical Engineering, Nanyang Technological University, Singapore 637459.

[2]Bioinformatics Institute, A*STAR, 30 Biopolis Street, Matrix, Singapore 138671.

[3]Singapore Eye Research Institute, Singapore 169856

[4]Frontiers Science Center for Flexible Electronics, Northwestern Polytechnical University, China 710072.

[5]Medical School of Ningbo University, China 315211.

[6]Department of Chemical Engineering, Massachusetts Institute of Technology, Cambridge, Massachusetts 02139, USA.
[7]Infectious Diseases Interdisciplinary Research Group, Singapore-MIT Alliance for Research and Technology (SMART), Singapore 138602.

[8]Department of Biological Sciences, National University of Singapore, Singapore 117558.

[9]School of Biological Sciences, Nanyang Technological University, Singapore 637551.

[10]Department of Chemistry and Biochemistry, University of California, Santa Barbara, CA 93106-9510, USA.

[11]Departments of Chemistry and Chemical & Biomolecular Engineering, National University of Singapore, Singapore 117543.

[12]Lee Kong Chian School of Medicine, Nanyang Technological University, Singapore 636921.

[13]School of Physical & Mathematical Sciences, Nanyang Technological University, Singapore 637371.

[#]The authors contributed equally.

*To whom correspondence should be addressed: M.B.C. (MBEChan@ntu.edu.sg) or K.P. (kevin.pethe@ntu.edu.sg) or G.C.B (chmbgc@nus.edu.sg)

Keywords: beta-peptide, antimicrobial peptides, Gram-selective, lipopolysaccharide, persisters, biofilm

Abstract

New antimicrobials are urgently needed to combat Gram-negative bacteria, particularly multi-drug resistant (MDR) and phenotypically resistant biofilm species. At present, only

sequence-defined alpha-peptides (*e.g.* polymyxin B) can selectively target Gram-negative bacterial lipopolysaccharides. We show that a copolymer, without a defined sequence, shows good potency against MDR Gram-negative bacteria including its biofilm form. The tapered blocky co-beta-peptide with controlled N-terminal hydrophobicity (#4) has strong interaction with the Gram-negative bacterial lipopolysaccharides via its backbone through electrostatic and hydrogen bonding interactions but not the Gram-positive bacterial and mammalian cell membranes so that this copolymer is non-toxic to these two latter cell types. The new #4 co-beta-peptide selectively kills Gram-negative bacteria with low cytotoxicity both *in vitro* and in a mouse biofilm wound infection model. This strategy provides a new concept for the design of Gram-negative selective antimicrobial peptidomimetics against MDR and biofilm species.

1. Introduction

No new antibiotic classes have been discovered for Gram-negative bacteria such as *Acinetobacter baumannii, Pseudomonas aeruginosa* and *Enterobacteriaceae* in the past 7 decades and in that time many resistant strains have evolved and spread in both clinical and community settings[1]. These Gram-negative bacteria are often recalcitrant to conventional antibiotic treatments, with rapid emergence of resistance to last-resort antibiotics[2]. Further, antibiotics are largely ineffective against persisters and biofilms as they target metabolically active bacteria. It is known that biofilm bacteria can be up to 1000 times more resistant to antibiotics than their planktonic forms [3, 4]. Further, biofilm, rather than planktonic bacteria are the relevant forms of colonization state of many clinically relevant infections, such as in chronic wounds, lung infections, urinary tract infections, *etc*[5]. It is worrisome that multi-drug resistance and biofilm phenotypes of Gram-negative bacteria have very limited treatment options.

Many works have been reported for selectively eradicating Gram-positive bacteria but no work has been published on MDR and biofilm Gram-negative bacteria[6-9]. Amongst the challenges to Gram-negative bacteria are their double membranes which makes them rather impenetrable. The Gram-negative bacterial outer membrane contains lipopolysaccharide (LPS) in the outer leaflet, forming a tight barrier that prevents the translocation of hydrophobic molecules through the impermeable outer membrane[10]. However, since LPS is the outermost layer of the Gram-negative bacterial envelope, it may be possible to achieve selective targeting of Gram-negative bacteria with rationally designed molecules that specifically target LPS molecules. LPS contains negatively charged lipids decorated with long chains of polysaccharides with phosphate and plentiful hydroxyl groups[11]. This suggests that molecules rich in their ability to engage in electrostatic and hydrogen bonding interactions hold the potential to selectively bind to LPS molecules. However, up to now, this principle of LPS targeting has not been translated. Even polymyxin B's (PMB) interaction with Gram-negative bacterial envelope is based on electrostatic and hydrophobic interaction with LPS and the displacement of divalent ions that hold the LPS together[12].

Beta-peptides are much less explored than natural alpha(α) antimicrobial peptides (AMPs) though they may be promising alternatives because their biological activity is similar to that of natural α-peptides with the added properties of being more resistant to proteolysis and commonly non-mutagenic[13-15]. Importantly, the existence of an extra carbon in the backbone of β-peptides allows them more compositional diversity than α-peptides. Despite advances in the synthetic chemistry of β-amino acids and peptides that make it possible to design and synthesize various antimicrobial β-peptides[7, 16-20], they have not been shown to selectively target Gram-negative bacteria over mammalian cells and Gram-positive bacteria, particularly their

biofilm forms. The most potent antimicrobial β-peptide yet synthesized is a poly(dimethyl β-lactam)-*co*-poly(cyclohexyl β-lactam) copolymer (P(DM-*co*-CH)) which has a tert-butylbenzoyl group at the N-terminus, but it has poor biocompatibility and no Gram-selectivity and has not been shown to have efficacy against biofilms[21].

Herein, we modulated the local terminal hydrophobicity of the P(DM-*co*-CH) co-β-peptide. Eight co-beta-peptides made from DM and CH residues, including the control (#1), and #2, #3 and #4-#8 co-beta-peptide, which are symmetric random, diblock, and controlled tapered blocky copolymers having different terminal compositions (**Scheme 1**). We found that the new co-beta-peptide (#4) with reduced N-terminal hydrophobicity shows strong potency against Gram-negative bacteria while having reduced/no potency against Gram-positive bacteria and mammalian cells. The #4 co-beta-peptide shows a high selectivity ratio against Gram-negative bacteria. Further, the new co-beta-peptide #4 eradicates the MDR Gram-negative bacteria biofilm in *in vitro* and *in vivo* wound tests and shows no toxicity in murine tests.

2. Results and Discussion

2.1. Synthesis and chemical characterization of copolymers.

Co-beta-peptide #2 to #3 were made using the co-initiator of terephthaloyl chloride via anionic ring-opening polymerization (AROP) of beta-lactam monomers under lithium bis(trimethylsilyl)amide (LiHMDS)-catalyzed conditions (**Scheme S1a and S1b)**. To make the co-β-peptides (#4) and (#5) where the N-terminal has reduced hydrophobicity, the protected amine and hydroxyl containing active ester of perfluorophenyl (tert-butoxycarbonyl)-glycinate(Boc-Gly-OPFP) and 2,5-dioxopyrrolidin-1-yl

2-(trityloxy)acetate (Trt-Glycolate-NHS) were prepared (**Scheme S2, Figure S1-S2)** and employed as the co-initiator (**Scheme S1c and S1e**). T-butylbenzoyl chloride was used as the co-initiator to prepare the control polymer having the bulky hydrophobic group of t-butylbenzoyl as the N-terminus (**Scheme S1d)**. Propionyl chloride, hexanoyl chloride and decanoyl chloride were used as the co-initiators to prepare polymers having different hydrophobicity in the N-terminus (**Scheme S1f-1h)**. The molecular structures of the obtained polymers were confirmed by NMR spectroscopy (**Figure S3-S10**). The degrees of polymerization of the polymers measured using GPC were 20 to 24 for polymers #1-#8, which were close to the monomer/initiator feed ratio of 20:1, and all polymers exhibited relatively narrow molecular weight distributions ($Đ$=1.20-1.34) (**Figure S11**). Circular dichroism (CD) spectroscopy measurement suggests that these beta-peptides do not self-assemble into stable secondary structures, even in the presence of bacterial or mammalian membranes (**Figure S12**).

2.2. Antimicrobial potency and biocompatibility.

The minimum inhibitory concentrations (MICs) of the synthesized β-peptides against a series of bacteria were evaluated. Consistent with previous report[21], #1 co-beta-peptide exhibited broad-spectrum antimicrobial potency (**Table 1 and Table 2**). However, the high toxicity of #1 co-beta-peptide against both erythrocytes (HC_{50}=312.5 μg/ml) and human kidney cells (HEK293) (IC_{50}=125 μg/ml) resulted in low selectivity indexes, *i.e.* (HC_{50}/MIC) of 19.5 and (IC_{50}/MIC) of 7.81, when tested against *E.coli* (**Table 1**). #2 co-beta-peptide had slightly improved HEK293 cell toxicity (IC_{50}=250 μg/ml) and hemolysis (HC_{50}=625 μg/ml) (**Table 1**). #3 co-beta-peptide was interestingly not hemolytic and less HEK293 cell toxic (HC_{50}=5000 μg/ml and IC_{50}=500 μg/ml) but it has lost its efficacy against Gram-positive bacteria and reduced efficacy against Gram-negative bacteria *E. coli* and *P. aeruginosa* (**Table 1**). With #4

co-beta-peptide, its efficacy against Gram-negative bacteria is preserved though the efficacy against Gram-positive bacteria is reduced (**Table 1 and Table 2**). The antimicrobial activity of #4 against *P. aeruginosa* PAO1 can be further enhanced to 4 μg/ml by 1 μg/ml polyimidazolium[22] (**Table S1**), which will be further explored in futures studies. Interestingly, #4 co-beta-peptide has significantly reduced toxicity against both erythrocytes (HC_{50}=5000 μg/ml) and human kidney cells (IC_{50}=500 μg/ml) giving the best selectivity index (HC_{50}/MIC =312.5 and IC_{50}/MIC= 31.25). Similar to #4, #5 maintained good antimicrobial activity towards Gram-negative bacteria while its toxicity towards both Gram-positive bacteria and mammalian cells was reduced (**Table 1**). To further explore the influence of N-terminal hydrophobicity, a series of β-peptide (#5-#8) with different hydrophobicity in N-terminus was prepared and evaluated. Interestingly, the selectively towards Gram-negative bacteria decreased with the increase in N-terminal hydrophobicity (**Table 1**). The increase in N-terminal hydrophobicity has a significant influence on their activity towards Gram-positive bacteria and mammalian cells, but has only a minor effect on Gram-negative bacteria. The reduction in N-terminal hydrophobicity also reduces their overall logP values (**Figure S13**). #4 and #5 with hydrophilic N-terminus have the relatively small logP values and the best selectivity. The #4 co-beta-peptide is one of our lead compounds with the highest selective index and was used for detailed characterization (The other lead compound with similar biological properties was #5).

With #4 co-beta-peptide, excellent antimicrobial activity was retained against various Gram-negative clinical isolates (**Table 2**), including carbapenem-resistant strains, with MICs against multi-drug resistant (MDR) *P. aeruginosa*, *A. baumannii* and *E. coli* ranging from 4 to 32 μg/ml. The potency of #4 co-beta-peptide against Gram-positive bacteria was lower than that of #1, which might result from the new polymer's reduced hydrophobicity at the N-terminus.

Further, #4 co-beta-peptide was stable after 24 h incubation with mouse blood plasma (**Table S2**), while the natural AMP melittin totally lost its potency, representing a significant improvement over classical antimicrobial alpha-peptide melittin as therapeutic agents.

#4 co-beta-peptide exhibited fast-killing kinetics against various multi-drug resistant (MDR) Gram-negative strains. At 2×MIC, it completely eradicated MDR *A. baumannii* MDRAB and *P. aeruginosa* PAER within 1 hour and MDR *E. coli* ECOR in 5 hours (**Figure 1**). The positive zeta potential value of #4 and the negative zeta potential values of bacteria suggest that the electrostatic interaction may be the initial driving force for association (**Figure 2a**). Indeed, bacteria treated with #4 show a trend of increasing zeta potential to more positive values with increasing concentration of polymer (**Figure 2a**), supporting that the electrostatic interaction is important. The antimicrobial activity of #4 was dramatically suppressed in the presence of LPS (**Figure 2b**), suggesting that it targets LPS molecules. Super-resolution stimulated emission depletion microscopy (STED) shows that rhodamine labelled #4 (Rho-#4) was mainly seen on the periphery of the bacteria (**Figure 2c**); superimposition of the red Rho-#4 and green membrane emissions results in bacterial images with an orange membrane (**Figure 2c**), indicating that the polymer was indeed adsorbed and resided in the bacterial membrane. Outer membrane and inner membrane permeabilization studies further show that #4 promotes the permeabilization of the bacterial outer and inner membranes (**Figure 2d-2g**). Cryo-TEM shows that, compared with the untreated *E. coli* K12 (**Figure 3a**) and *P. aeruginosa* PAO1 (**Figure 3c**) that have intact membranes, substantial wrinkling and lysis occurred in the membranes of #4 treated *E. coli* K12 (**Figure 3b**) and *P. aeruginosa* PAO1 (**Figure 3d**). Furthermore, #4 treated bacteria did not show an obvious increase in ROS signal compared to untreated bacteria control (**Figure S14a, S14b and Figure S15**) and the antimicrobial potency of the polymer was not

affected in the presence of the ROS quencher N-acetyl-L-cysteine (NAC) (**Figure S14c**). These results suggest that ROS generation does not contribute to the antimicrobial activity of the polymer.

2.3. Copolymerization kinetics and polymer structure.

For #4 co-beta-peptide, the copolymerization using Boc-Gly-OPFP as the new co-initiator was tracked using gas chromatography (GC) following a reported procedure[21]. The hydrophobic cyclohexyl (CH) beta-lactam monomers were found to be consumed faster than the cationic dimethyl (DM) beta-lactam monomers (**Figure S16**), indicating that the N-terminus of #4 was significantly richer in the hydrophobic (CH) residues while the C-terminus was richer in the cationic (DM) residues (**Figure 4**), which is similar to the reported distribution of DM and CH residues in #1 using t-butylbenzoyl chloride as the co-initiator[21]. The faster copolymerization of CH versus DM results in a tapered blocky structure in the resulting co-beta-peptides with a greater accumulation of the hydrophobic CH units at the N-terminals. Replacement of the bulky hydrophobic residual N-terminal group t-butylbenzoyl (LogP=3.43) in #1 with a highly hydrophilic ammonium group (LogP=-3.20) from the new co-initiator (Boc-Gly-OPFP) for #4 would significantly decrease the local hydrophobicity at the N-terminus of the new co-beta-peptide (**Figure 4b**). The higher hydrophobicity near the N-terminus in #1 compared to #4 was supported by dynamic light scattering (DLS) measurements in phosphate-buffered saline (PBS) solution; the critical aggregation concentration (CAC) of #1 is about 0.5 mg/mL and the hydrodynamic radius of this polymer increased significantly at concentration above 0.5 mg/mL while #4 remained as solvated single polymer chains up to 16 mg/mL (**Figure S17**).

2.4. Isothermal titration calorimetry and interaction with model liposomes.

To delineate the interaction force of the beta-peptides at the molecular level with the three cell types, isothermal titration calorimetry (ITC) was applied to study the interaction of #1 versus #4 with liposome models of the mammalian plasma membrane (POPC)[23], Gram-positive cytoplasmic membrane (POPG)[7] and Gram-negative bacterial outer membrane (LPS)[24]. The ITC titration thermograms are shown in supplementary **Figure S18** and the derived thermodynamic interaction parameters are shown in **Table 3**. The #1 (control) strongly interacted with all 3 liposomes (mammalian model liposome (ΔG=-25.1 kJ/mol, K_A=16694 M^{-1}), Gram-positive bacteria model liposome (ΔG=-25.7 kJ/mol, K_A=21459 M^{-1}) and Gram-negative LPS liposome (ΔG=-26.3 kJ/mol, K_A=26954 M^{-1}) (**Table 3, Figure S18a(i)**, **18b(i) and 18c(i)**), which corroborates its non-selective toxicity to all three types of cells. The #1 displayed slightly unfavourable (positive) enthalpic interactions with both the mammalian model liposome (ΔH=1.04 kJ/mol) and Gram-positive model liposome (ΔH=3.68 kJ/mol). However, the #1 showed a large favorable (positive) entropic gain with the mammalian (ΔS =84.2 J/mol/K) and Gram-positive liposomes (ΔS =94.7 J/mol/K), which may arise from the release of ordered water molecules, as well as the decrease in lipid order, during the penetration of the tert-butylbenzoyl group into the mammalian and bacterial cytoplasmic membrane. So the control peptide interaction with mammalian and Gram-positive cells is hydrophobic-driven. The #1 binding with the Gram-negative LPS is an exothermic process (ΔH=-50.2 kJ/mol), indicating that the heat release associated with the electrostatic interaction and hydrogen bonds between the cationic groups of the β-peptide and phosphate groups of LPS was larger than the unfavorable entropic contribution (ΔS =-77.4 J/mol/K) which is probably associated with desolvation (excluding the surrounding water molecules around LPS) and lipid perturbation. Hence, the control β-peptide

(#1) interactions with mammalian cells, Gram-positive bacteria and Gram-negative bacteria are respectively governed by entropic, entropic, and enthalpic interactions (**Table 3**).

To prove that our new copolymer (#4) has different interaction forces that will lead to selectivity, we also carried out the ITC studies. We found that #4 showed no interaction with the mammalian model liposome and weak interaction with Gram-positive model liposome (ΔG=-22.0 kJ/mol, K_A=5076 M^{-1}), but strong interaction with Gram-negative LPS (ΔG=-26.5 kJ/mol, K_A=29325 M^{-1}) (**Table 3, Figure S18a(ii)**, **18b(ii) and 18c(ii)**), which is consistent with its observed selectivity towards Gram-negative bacteria. With the new #4 peptide, the ITC measurements with the mammalian model liposome did not show any detectable heat flow (**Table 3**, **Figure S18a(ii)**), suggesting no interaction of #4 with the mammalian membrane, which is consistent with its low toxicity against mammalian cells. With the Gram-positive model liposome, the titration of #4 results in relatively weak but still favorable affinity (ΔG=-22.0 kJ/mol, K_A=5076 M^{-1}), which is consistent with its weak antimicrobial potency against Gram-positive bacteria. The #4 interaction with the Gram-positive bacteria is governed by entropic interaction (ΔS =82.1 J/mol/K), which is attributed to water displacement. However, the interaction of #4 with Gram-negative LPS (ΔG=-26.5 kJ/mol, K_A=29325 M^{-1}) is much more favorable than with mammalian cell and Gram-positive bacteria. The #4 interaction with LPS is driven by enthalpic interaction, and a large enthalpy release (ΔH=-48.6 kJ/mol) was observed, which is probably due to electrostatic interactions and the formation of hydrogen bonds between the peptide amine and LPS phosphate groups. In the case of the Gram-negative inner membrane model liposome, although the titration of #4 is still favourable (ΔG=-14.8 kJ/mol, K_A=311 M^{-1}) (**Figure S19**), the interaction is weaker than with the outer membrane, supporting the view that #4 mainly targets the outer membrane. Gram-positive bacteria have anionic lipoteichoic acid

(LTA) in the outer layer of the bacterial membrane, but it only covers around 10% Gram-positive bacterial membrane[25], whereas LPS covers around 75% Gram-negative bacterial outer membrane[26, 27]. In addition to the lower abundance of LTA in the bacterial membrane, #4 polymers have a relatively weaker interaction with Gram-positive bacterial LTA (K_A=12364 M^{-1}) (**Figure S20**) compared to Gram-negative bacterial LPS (K_A=29325 M^{-1}). Similar to #4, #5 also showed no interaction with the mammalian model liposome and weak interaction with Gram-positive model liposome (ΔG=-23.0 kJ/mol, K_A=7518 M^{-1}) (**Figure S21a and S21b**), but strong interaction with Gram-negative outer membrane LPS (ΔG=-28.2 kJ/mol, K_A=57803 M^{-1}) (**Figure S21c**), all of which is consistent with its observed selectivity towards Gram-negative bacteria.

In summary, for the control #1 peptide interaction with the mammalian and Gram-positive model liposomes, the positive entropy changes (which are favorable), together with positive enthalpy changes (which are unfavorable), indicate that the binding of this β-peptide to the two membranes was driven by entropy due to hydrophobic insertion[28]. A change of the bulky hydrophobic tert-butylbenzoyl group at the N-terminus of the control #1 beta-peptide to the hydrophilic ammonium makes the new #4 peptide insufficiently hydrophobic to permit strong interaction with mammalian cell membrane and with Gram-positive cytoplasmic membrane. The interactions of both β-peptides with LPS are driven by enthalpic effects resulting from electrostatic and hydrogen bonding interactions[29], which were unchanged for the two peptides. The selectivity of #4 is achieved through retention of enthalpic interactions with Gram-negative LPS coupled with removal/reduction of entropic interactions with mammalian and Gram-positive membranes.

2.5. Molecular dynamics simulations.

To gain further insights into the mechanism of action of these β-peptides with the different membranes at the atomic level, we carried out molecular dynamics (MD) simulations of #1 and #4 with model membranes of mammalian cells, Gram-positive bacteria and Gram-negative bacteria. We first simulated the modes of interaction of #1 and #4 with a model POPC bilayer mimicking the mammalian membrane[23]. **Figure 5a(i)** and **5a(ii)** show snapshots of the two β-peptide interactions with the model mammalian membrane. As the simulation progresses, with the control #1 peptide, the N-terminal (orange peptide terminal) penetrates into the interior of the bilayer (**Figure 5a(i)**) and the distance between the N-terminal residue and lipid bilayer center gradually decreases (**Figure S22a**). The final distance of the N-terminal from the bilayer center is around 0 nm, corresponding to the bilayer center. The C-terminal segment of the #1 still locates at the head group region, forming an amphiphilic conformation that enables #1 to perturb both head groups and lipid tails (**Figure 5a(i)**). In contrast with the #4 peptide, due to its lack of hydrophobic groups at the N-terminus, #1 primarily locates at the head group region of the membrane without insertion (**Figure 5a(ii), Figure S22a**), suggesting low membrane perturbation. We conclude that the toxicity of #1 (control) towards mammalian membrane mainly originates from the hydrophobic insertion of the tert-butylbenzoyl group into the membrane, which is entropically driven (**Table 3**).

We subsequently examined the modes of interaction of the two β-peptides with a model Gram-positive cytoplasmic membrane consisting of POPG lipids[7]. **Figure 5b(i)** shows that the N-terminal segment of #1 (orange) also penetrates into the lipid tail region of the bacterial cytoplasmic membrane (**Figure S22b**), while the C-terminal segment locates at the head group

region, demonstrating a mode of interaction of the control peptide similar to the case of mammalian membrane. For #4, both the N-terminal and C-terminal segments of the new β-peptides were found to stay on the membrane surface without penetration during the entire simulation (**Figure 5b(ii), Figure S22b**), suggesting low activity of the new peptide against the Gram-positive bacterial cytoplasmic membrane. It is known that the water molecules around a hydrophobic surface have restricted freedom[30]. Upon penetration into the membrane, the dehydration of the hydrophobic groups restores the translational and orientational degrees of freedom of the surface water molecules, which results in an entropy gain corroborated by the ITC measurements. Because of the high hydrophobicity at the N-terminus of #1, the control peptide experiences a much larger entropy gain than does #4, which is consistent with the ITC results (**Table 3**).

To further understand the action mechanism against Gram-negative bacteria, we carried out MD simulations of the two β-peptides with a model lipid A, an essential component of LPS, bilayer mimicking the outer membrane of Gram-negative bacteria[31]. It has been shown that lipid A membrane is stabilized by divalent cations that are involved in salt-bridges with the phosphate groups of the membrane[31]. **Figure 5c(i)-5c(ii)** and **Figure S22c-22f** show that both peptides destabilize the lipid A membrane in a similar manner and release the divalent Ca^{2+} (yellow spheres). As both peptides are cationic and the lipid A membrane is anionic, it is the electrostatic interactions that steer the β-peptides to the membrane. Upon adsorption onto the membrane, the amine groups in the side chains start to engage in hydrogen bonding with the phosphate groups (**Figure 5d(i)-5d(ii)**), resulting in the disruption of the salt-bridges and release of calcium ions from the membrane surface. As both the electrostatic interactions and the formation of amine-phosphate hydrogen bonds are exothermic, the binding of the peptide to LPS results in

significant enthalpy release. As the simulation progresses, the membrane is significantly distorted, with some lipid tails becoming exposed to the aqueous phase. The hydration of the exposed lipid tails has to pay an entropic penalty, consistent with the entropy loss (ΔS=-77.4 J/mol/K and ΔS=-70.4 J/mol/K, respectively) observed in the ITC experiments (**Table 3**). To study the influence of ammonium N-terminus, molecular dynamistic simulation of #5 with different model membranes was also carried out. Similar to #4, #5 only locates at the head group region of the mammalian and Gram-positive membrane without insertion due to the lack of hydrophobic groups at the N-terminus (**Figure 5a(iii), 5b(iii), Figure S22a, S22b**). In the case of Gram-negative bacterial membrane, the electrostatic interactions steer #5 to the membrane (**Figure S22g, S22h**). Upon adsorption onto the membrane, the amine groups in the side chains of #5 start to engage in hydrogen bonding with the phosphate groups (**Figure 5d(iii)**), resulting in the disruption of the salt-bridges and release of calcium ions from the membrane surface (**Figure 5c(iii)**), which eventually leads to significant membrane perturbations.

2.6. The #4 co-beta-peptide has activity against Gram-negative persisters and biofilm and low resistance.

Bacteria become tolerant of conventional antibiotic treatment by either generating genetic mutants (resistance)[32] or going into a dormant state (persister cells)[33]. Persister cells are a special state of bacteria with inactive metabolism and are mostly un-treatable by classical antibiotics, which usually eradicate only metabolically active cells [34, 35]. #4 killed persister *A. baumannii* ATCC 19606 at 1× its MIC (**Figure 6a**), whereas the conventional antibiotic gentamicin was totally ineffective at concentrations as high as 64× its MIC (**Figure 6b**). We further demonstrated that #4 eradicated more than 99% of biofilm-associated *A. baumannii*

ATCC19606 and MDR clinical isolate MDRAB (**Figure 6c-6d**), indicating that this class of antibacterial may prevent infection relapse by targeting both persisters and biofilm-associated subpopulations. Consistent with biofilm-killing study, #4 treated bacterial biofilm showed a huge number of dead bacterial cells compared to the untreated control **(Figure 6e**). We found that with repeated sub-inhibitory dosing of #4, the MIC increased by only 2-fold for 10 to 18 passages, while ciprofloxacin showed a 2048-fold increase in MIC (**Figure 7**). We attempt to generate spontaneous mutants of *E. coli* K12 to #4 but were unsuccessful, giving a frequency of resistance of less than 4.4×10^{-9}, which is less than that of the conventional antibiotic ciprofloxacin. These results indicate that #4 does not rapidly elicit the emergence of resistance.

2.7. *In vivo* biocompatibility and efficacy against biofilm.

The #4 copolymer was tested *in vivo* in a murine wound biofilm model. Biofilm of the multi-drug resistant (MDR) clinical isolate *A. baumannii* MDRAB was created at the murine excisional wound by infecting the wound with the bacteria for 24 hours, so that bacterial biofilm was established. The treatment with #4 reduced the bacterial burden by more than 99.2% in the wound areas, which was superior to the last-resort antibiotic meropenem (**Figure 8**). To measure the *in vivo* murine toxicity, #4 was injected via the tail vein at a dosage of 10 mg/kg body weight, and the mouse condition was continuously monitored for 7 days. At 7 days post-injection, all the mice were alive and active. No obvious illness or lassitude was found in visual observation of the mice. The levels of biomarkers related to liver and kidney function and electrolyte balance did not show significant change at 24 h and 7 days after intravenous injection (**Table S3**). The data indicate that #4 could treat the MDR Gram-negative biofilm and did not cause acute toxicity to the liver and kidney or influence the blood chemistry.

2.8. Discussion.

We have discovered important differences in the interactions of these beta-peptides with the three cell types. The #4 with controlled N-terminal hydrophobicity has the best biocompatibility profile while retaining good efficacy against Gram-negative bacteria. The interactions of the two tapered blocky co-peptides (#1 and #4) with Gram-negative bacterial LPS are driven by the peptide backbone interactions via electrostatic interaction and hydrogen bonding with the LPS phosphate groups. On the other hand, the interactions of the co-peptides with Gram-positive bacteria and mammalian cells are driven by the peptide N-terminal segment hydrophobicity. The modest structural change at the N-terminal from the bulky hydrophobic tert-butylbenzoyl group of the highly potent but toxic original β-peptide (#1) to a hydrophilic ammonium group for the new co-beta-peptide (#4) significantly improved biocompatibility without sacrificing potency against multiple Gram-negative bacteria. Changing the co-initiator residue from the tert-butylbenzoyl to the ammonium group significantly reduced the local hydrophobicity at the N-terminus as well as the global amphiphilicity of the entire β-peptide.

The few peptides/antibiotics that are selective against Gram-negative bacteria include PMB and darobactin[12, 36, 37]. PMB, a sequence-dependent peptide, selectively kills Gram-negative bacteria by targeting the LPS molecules via electrostatic and hydrophobic interactions[12]. However, the hydrophobic lipid tail in PMB also imparts toxicity[38]. The depletion of hydrophobic lipid tail in PMB caused its loss of antimicrobial potency against Gram-negative bacteria[39]. Darobactin selectively kills Gram-negative bacteria by targeting the β-barrel assembly machinery (Bam)A, an outer membrane protein[36]. However, darobactin-resistant bacteria have emerged after only a few passages, which is possibly due to the fact that it targets a

specific protein that is easily mutated. In contrast to PMB, the #4 β-peptide copolymer made by copolymerization is not sequence-dependent and can be made in large scale at low cost. Further, our copolymer that interacts with LPS via electrostatic and hydrogen bonding interactions has reduced toxicity associated with the non-selective hydrophobic interaction with mammalian cells. As #4 targets the general structure of the outer membrane of Gram-negative bacteria, the frequency of spontaneous resistance is low.

Biofilms are aggregates of microorganisms in which the microorganisms are embedded in a self-produced matrix of extracellular polymeric substances (EPSs)[40, 41]. The US National Institutes of Health has attributed more than 80% of human infections to be biofilm-related[42]. Metabolically dormant persister bacteria which are present in biofilms are intrinsically tolerant to antibiotics[33, 43]. However, persisters still need an intact membrane for survival. They are vulnerable to agents that can perturb or disrupt membrane integrity or function, making the membrane an ideal target for the treatment of persisters[44]. The efficacy of #4 against Gram-negative persisters and biofilm is attributable to its ability to interact with the outer membrane constituent LPS. Small cationic polymers/peptides are able to penetrate deep into biofilms[45], thus #4 successfully removes biofilm bacteria by attacking persisters in the deep layers of the biofilm. It offers an option for treating the Gram-negative bacterial biofilms not easily treatable with antibiotics.

3. Conclusion

We have designed and synthesized a new biocompatible β-peptide copolymer (#4) with controlled terminal hydrophobicity that selectively eradicates Gram-negative bacteria without cytotoxicity towards mammalian cells. This is the first report of a copolymer that is not

sequence-defined that shows Gram-negative LPS selectivity. We showed that both the control and new copolymers have tapered blocky backbones that are able to intimately interact via electrostatic and hydrogen bonding with the phosphate head groups of Gram-negative LPS, without the need for a hydrophobic interaction driving force. To minimize local hydrophobicity that leads to toxicity to mammalian cells, we used a new co-initiator that leaves behind a hydrophilic ammonium group at the N-terminus of the tapered blocky copolymer. The decreased local hydrophobicity at the N- terminus of the new #4 copolymer results in reduced hydrophobic interactions with both mammalian cells and Gram-positive bacteria. The excellent *in vitro* bactericidal activity against carbapenem-resistant *A. baumannii* MDRAB, the most critical pathogen in the WHO list, was demonstrated in an *in vivo* mouse biofilm study. The design of tapered blocky co-beta-peptides without global amphiphilicity (*i.e.* molecules with low local hydrophobicity) and high propensity to engage in electrostatic and hydrogen bonding interactions with LPS provides a new approach for the design of non-toxic Gram-negative selective agents.

Acknowledgments

This research is supported by the Ministry of Education, Singapore, under its MOE AcRF Tier 3 Awards of MOE2018-T3-1-003 and MOE2013-T3-1-002. Zhangyong Si acknowledges the support of an NTU Ph.D. scholarship. The authors thank the NSCC and ASTAR ACRC for providing the computational resources to perform simulations and A*STAR for support (grant IDs H17/01/a0/010, IAF111213C). We also thank the A*STAR Wound Care Innovation for the Tropics IAF-PP (HBMS Domain) with grant number H17/01/a0/0M9, the A*STAR RIE2020 Advanced Manufacturing and Engineering (AME) IAP-PP Specialty Chemicals Programme (Grant No. A1786a0032) and A*STAR Career Development Award (CDA, Grant No. 202D8155),

the Major Project of 2025 Sci &Tech Innovation of Ningbo, China (2018B10052) and NTU for funding support.

Author contributions

M.B.C. supervised and guided the overall research; Z.S. and M.B.C. conceived the project. Z.S. synthesized the poly(beta-peptides). J.L. carried out the MD simulations and analyzed the data in discussions with CSV. L.R., R. S. and O.Y.J. conducted the *in vitro* biological tests. Z.S. conducted the *in vivo* tests. Y.Z. supervised *in vivo* toxicity tests. K.P. and P.T.H. co-supervised the biology testing and interpretation. G.C.B. and P. L. co-supervised the chemical synthesis and characterization. Z.S., K.P., G.C.B and M.B.C. wrote the manuscript with contributions from the other authors.

Competing financial interests

The authors declare no competing financial interests. CSV is the founder of Sinopsee Therapeutics, a biotechnology company developing molecules for therapeutic purposes; the current work has no conflict with the company.

Data availability.

Data supporting the findings of this study are available in this article and its supplementary information file.

References

[1] Si Z, Zheng W, Prananty D, Li J, Koh CH, Kang E-T, et al. Polymers as advanced antibacterial and antibiofilm agents for direct and combination therapies. Chemical Science. 2022;13:345-64.
[2] Control CfD, Prevention. Antibiotic Resistance Threats in the United States 2019, Atlanta, GA: US Department of Health and Human Services, CDC; 2019.
[3] Sharma D, Misba L, Khan AU. Antibiotics versus biofilm: an emerging battleground in microbial communities. Antimicrobial Resistance & Infection Control. 2019;8:1-10.
[4] Bi Y, Xia G, Shi C, Wan J, Liu L, Chen Y, et al. Therapeutic strategies against bacterial biofilms. Fundamental Research. 2021;1:183-212..
[5] Lebeaux D, Ghigo J-M, Beloin C. Biofilm-related infections: bridging the gap between

clinical management and fundamental aspects of recalcitrance toward antibiotics. Microbiology and Molecular Biology Reviews. 2014;78:510-43.
[6] Li J, Zhang K, Ruan L, Chin SF, Wickramasinghe N, Liu H, et al. Block copolymer nanoparticles remove biofilms of drug-resistant gram-positive bacteria by nanoscale bacterial debridement. Nano letters. 2018;18:4180-7.
[7] Zhang K, Du Y, Si Z, Liu Y, Turvey ME, Raju C, et al. Enantiomeric glycosylated cationic block co-beta-peptides eradicate Staphylococcus aureus biofilms and antibiotic-tolerant persisters. Nature communications. 2019;10:1-14.
[8] Zhou M, Qian Y, Xie J, Zhang W, Jiang W, Xiao X, et al. Poly (2 - Oxazoline) - based functional peptide mimics: Eradicating MRSA infections and persisters while alleviating antimicrobial resistance. Angewandte Chemie International Edition. 2020;59:6412-9.
[9] Xie J, Zhou M, Qian Y, Cong Z, Chen S, Zhang W, et al. Addressing MRSA infection and antibacterial resistance with peptoid polymers. Nature Communications. 2021;12:5898.
[10] Leitgeb B, Szekeres A, Manczinger L, Vágvölgyi C, Kredics L. The history of alamethicin: a review of the most extensively studied peptaibol. Chemistry & biodiversity. 2007;4:1027-51.
[11] Di Lorenzo F, Duda KA, Lanzetta R, Silipo A, De Castro C, Molinaro A. A Journey from Structure to Function of Bacterial Lipopolysaccharides. Chemical Reviews. 2021;122:15767-15821.
[12] Srimal S, Surolia N, Balasubramanian S, Surolia A. Titration calorimetric studies to elucidate the specificity of the interactions of polymyxin B with lipopolysaccharides and lipid A. 1996;315:679.
[13] Goodman CM, Choi S, Shandler S, DeGrado WF. Foldamers as versatile frameworks for the design and evolution of function. Nature chemical biology. 2007;3:252-62.
[14] Cheng RP, Gellman SH, DeGrado WF. β-Peptides: from structure to function. Chemical reviews. 2001;101:3219-32.
[15] Chen Q, Zhang D, Zhang W, Zhang H, Zou J, Chen M, et al. Dual mechanism β-amino acid polymers promoting cell adhesion. Nature communications. 2021;12:1-13.
[16] Porter EA, Wang X, Lee H-S, Weisblum B, Gellman SH. Non-haemolytic β-amino-acid oligomers. Nature. 2000;404:565-.
[17] Dane EL, Ballok AE, O'Toole GA, Grinstaff MW. Synthesis of bioinspired carbohydrate amphiphiles that promote and inhibit biofilms. Chemical science. 2014;5:551-7.
[18] Zhou M, Xiao X, Cong Z, Wu Y, Zhang W, Ma P, et al. Water - Insensitive Synthesis of Poly - β - Peptides with Defined Architecture. Angewandte Chemie International Edition. 2020;59:7240-4.
[19] Si Z, Lim HW, Tay MY, Du Y, Ruan L, Qiu H, et al. A Glycosylated Cationic Block Poly (β - peptide) Reverses Intrinsic Antibiotic Resistance in All ESKAPE Gram - Negative Bacteria. Angewandte Chemie International Edition. 2020;59:6819-26.
[20] Liu L, Courtney KC, Huth SW, Rank LA, Weisblum B, Chapman ER, et al. Beyond Amphiphilic Balance: Changing Subunit Stereochemistry Alters the Pore-Forming Activity of Nylon-3 Polymers. Journal of the American Chemical Society. 2021;143:3219-30.
[21] Liu R, Chen X, Chakraborty S, Lemke JJ, Hayouka Z, Chow C, et al. Tuning the biological activity profile of antibacterial polymers via subunit substitution pattern. Journal of the American Chemical Society. 2014;136:4410-8.
[22] Zhong W, Shi Z, Mahadevegowda SH, Liu B, Zhang K, Koh CH, et al. Designer broad-spectrum polyimidazolium antibiotics. Proceedings of the National Academy of Sciences. 2020;117:31376-85.

[23] Hou Z, Shankar YV, Liu Y, Ding F, Subramanion JL, Ravikumar V, et al. Nanoparticles of short cationic peptidopolysaccharide self-assembled by hydrogen bonding with antibacterial effect against multidrug-resistant bacteria. ACS applied materials & interfaces. 2017;9:38288-303.
[24] Srimal S, Surolia N, Balasubramanian S, Surolia A. Titration calorimetric studies to elucidate the specificity of the interactions of polymyxin B with lipopolysaccharides and lipid A. Biochemical journal. 1996;315:679-86.
[25] Malanovic N, Lohner K. Antimicrobial peptides targeting gram-positive bacteria. Pharmaceuticals. 2016;9:59.
[26] Jacobson KH, Gunsolus IL, Kuech TR, Troiano JM, Melby ES, Lohse SE, et al. Lipopolysaccharide density and structure govern the extent and distance of nanoparticle interaction with actual and model bacterial outer membranes. Environmental science & technology. 2015;49:10642-50.
[27] Osborn M, Rosen S, Rothfield L, Zeleznick L, Horecker B. Lipopolysaccharide of the Gram-Negative Cell Wall: Biosynthesis of a complex heteropolysaccharide occurs by successive addition of specific sugar residues. Science. 1964;145:783-9.
[28] Uppu D, Konai M, Baul U, Singh P, Siersma T, Samaddar S, et al. Isosteric substitution in cationic-amphiphilic polymers reveals an important role for hydrogen bonding in bacterial membrane interactions. Chemical science. 2016;7:4613-23.
[29] Abraham T, Lewis RN, Hodges RS, McElhaney RN. Isothermal titration calorimetry studies of the binding of a rationally designed analogue of the antimicrobial peptide gramicidin s to phospholipid bilayer membranes. Biochemistry. 2005;44:2103-12.
[30] Galamba N. Water's structure around hydrophobic solutes and the iceberg model. The Journal of Physical Chemistry B. 2013;117:2153-9.
[31] Li J, Beuerman R, Verma CS. Mechanism of polyamine induced colistin resistance through electrostatic networks on bacterial outer membranes. Biochimica et Biophysica Acta (BBA)-Biomembranes. 2020:183297.
[32] Blair JM, Webber MA, Baylay AJ, Ogbolu DO, Piddock LJ. Molecular mechanisms of antibiotic resistance. Nature Reviews Microbiology. 2015;13:42.
[33] Fisher RA, Gollan B, Helaine S. Persistent bacterial infections and persister cells. Nature Reviews Microbiology. 2017;15:453.
[34] Allison KR, Brynildsen MP, Collins JJ. Metabolite-enabled eradication of bacterial persisters by aminoglycosides. Nature. 2011;473:216.
[35] Kim W, Zhu W, Hendricks GL, Van Tyne D, Steele AD, Keohane CE, et al. A new class of synthetic retinoid antibiotics effective against bacterial persisters. Nature. 2018;556:103.
[36] Imai Y, Meyer KJ, Iinishi A, Favre-Godal Q, Green R, Manuse S, et al. A new antibiotic selectively kills Gram-negative pathogens. Nature. 2019;576:459-464..
[37] Kaur H, Jakob RP, Marzinek JK, Green R, Imai Y, Bolla JR, et al. The antibiotic darobactin mimics a β-strand to inhibit outer membrane insertase. Nature. 2021:1-5.
[38] Vaara M. Polymyxin derivatives that sensitize Gram-negative bacteria to other antibiotics. Molecules. 2019;24:249.
[39] French S, Farha M, Ellis MJ, Sameer Z, Côté J-P, Cotroneo N, et al. Potentiation of antibiotics against Gram-negative bacteria by polymyxin B analogue SPR741 from unique perturbation of the outer membrane. ACS infectious diseases. 2019;6:1405-12.
[40] Flemming H-C, Wingender J, Szewzyk U, Steinberg P, Rice SA, Kjelleberg S. Biofilms: an emergent form of bacterial life. Nature Reviews Microbiology. 2016;14:563.

[41] Blackman LD, Qu Y, Cass P, Locock KE. Approaches for the inhibition and elimination of microbial biofilms using macromolecular agents. Chemical Society Reviews. 2021;50:1587-1616.
[42] Houry A, Gohar M, Deschamps J, Tischenko E, Aymerich S, Gruss A, et al. Bacterial swimmers that infiltrate and take over the biofilm matrix. Proceedings of the National Academy of Sciences. 2012;109:13088-93.
[43] Koo H, Allan RN, Howlin RP, Stoodley P, Hall-Stoodley L. Targeting microbial biofilms: current and prospective therapeutic strategies. Nature Reviews Microbiology. 2017;15:740-55.
[44] Defraine V, Fauvart M, Michiels J. Fighting bacterial persistence: Current and emerging anti-persister strategies and therapeutics. Drug Resistance Updates. 2018;38:12-26.
[45] Pfalzgraff A, Brandenburg K, Weindl G. Antimicrobial peptides and their therapeutic potential for bacterial skin infections and wounds. Frontiers in pharmacology. 2018;9:281.

Scheme, Figures and Tables

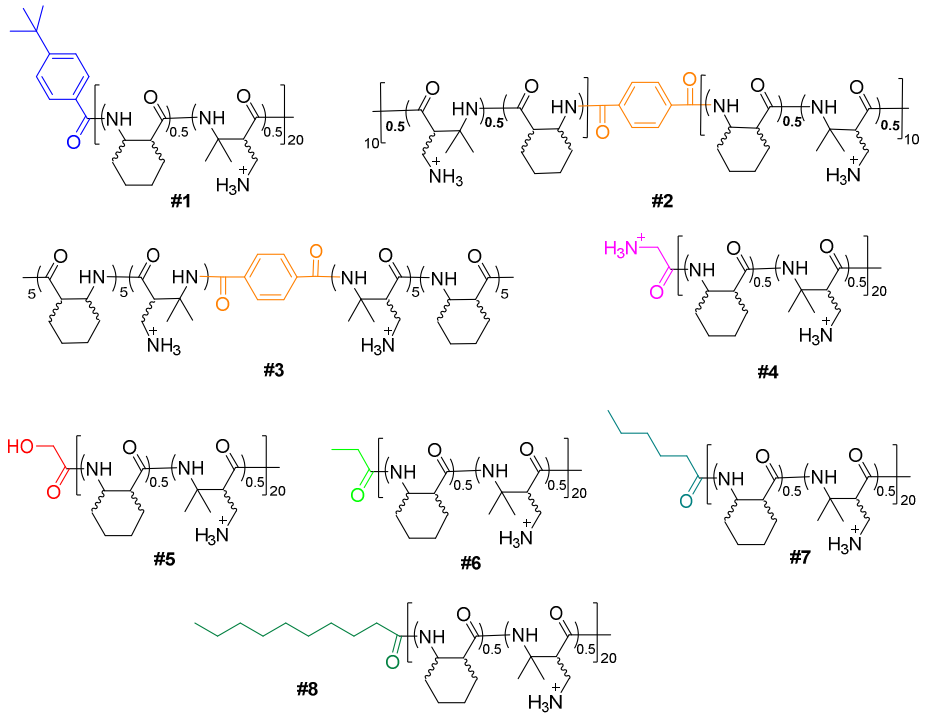

Scheme 1. The chemical structures of different β-peptides.

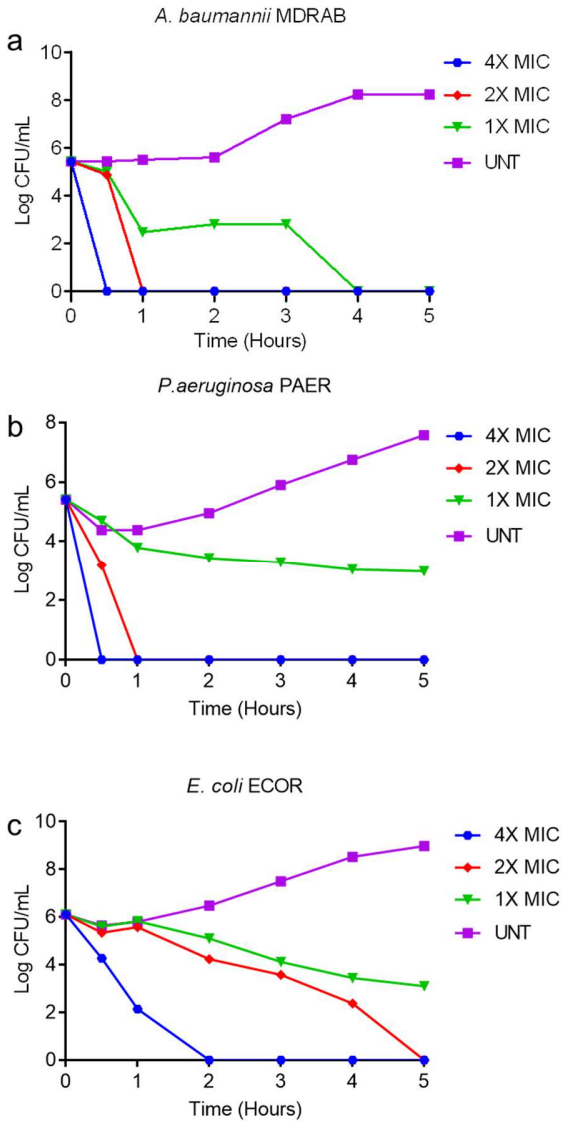

Figure 1. Kill kinetics of #4 against multi-drug resistant Gram-negative clinical isolates (a) *A. baumannii* MDRAB, (b) *P. aeruginosa* PAER and (c) *E. coli* ECOR at 1×, 2× and 4× MICs of polymer addition.

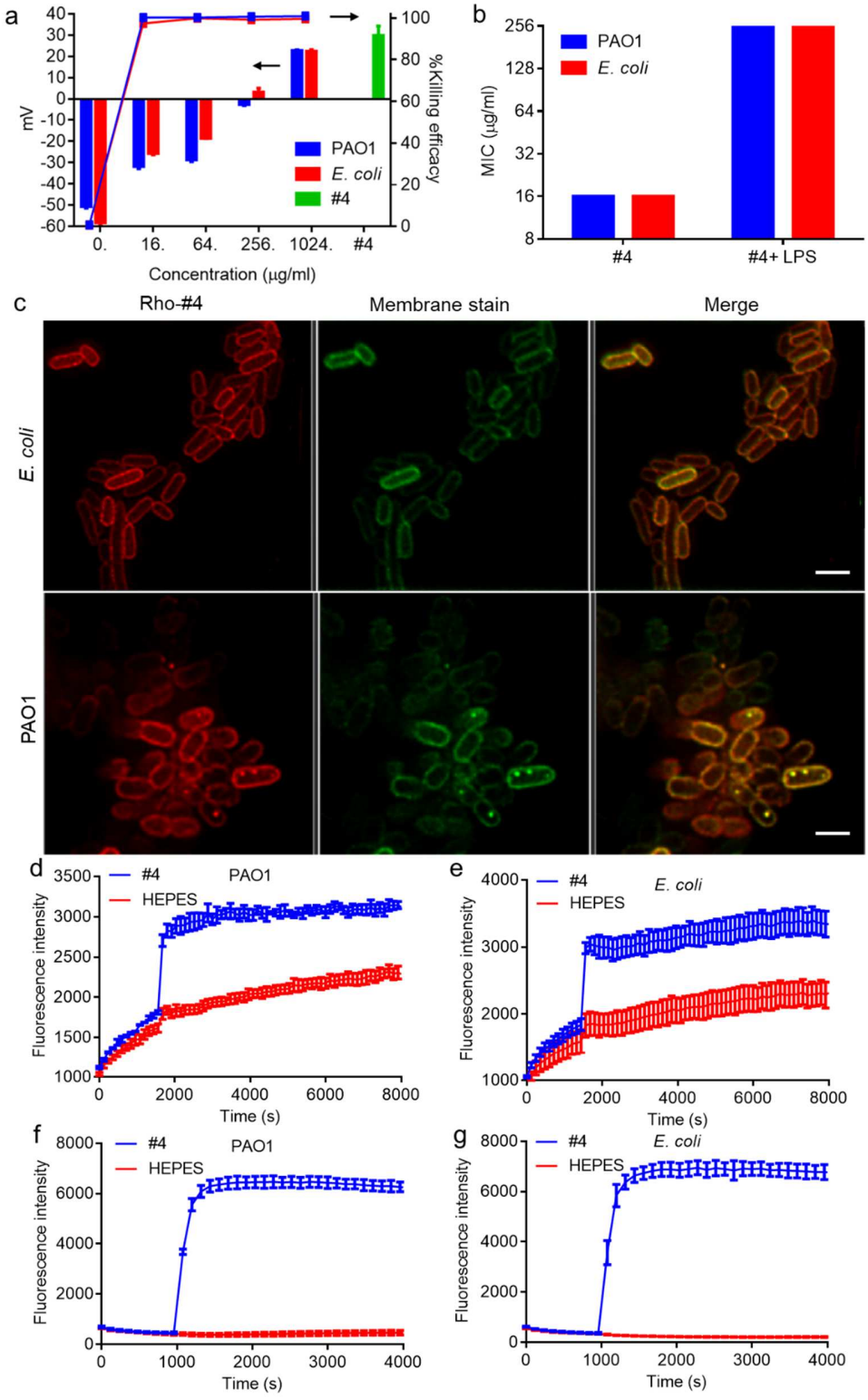

Figure 2. (a) Zeta potential values of bacteria, #4 and bacteria treated with different concentrations of #4, as well as their killing efficacy. (b) The antimicrobial activity of #4 alone

and #4 in the presence of LPS (500 µg/ml). (c) Super resolution STED microscopy images of *E. coli* 8739 and *P. aeruginosa* PAO1 treated with 1×MIC Rho-#4 (red); bacterial membrane was stained with FM1-43FX (green), scale bar 2 µm. (d) and (e) 1×MIC #4 triggers a significant increase in outer-membrane permeability of *P. aeruginosa* PAO1 (d) and *E. coli* 8739 (e) using1-N-phenylnaphthylamine (NPN) as an indicator of outer membrane permeability. (f) and (g) 1×MIC #4 triggers a significant increase inner membrane permeability of *P. aeruginosa* PAO1 (f) and *E. coli* 8739 (g) using 3,3'-Dipropylthiadicarbocyanine iodide ($DiSC_3(5)$) as an indicator of inner membrane permeability.

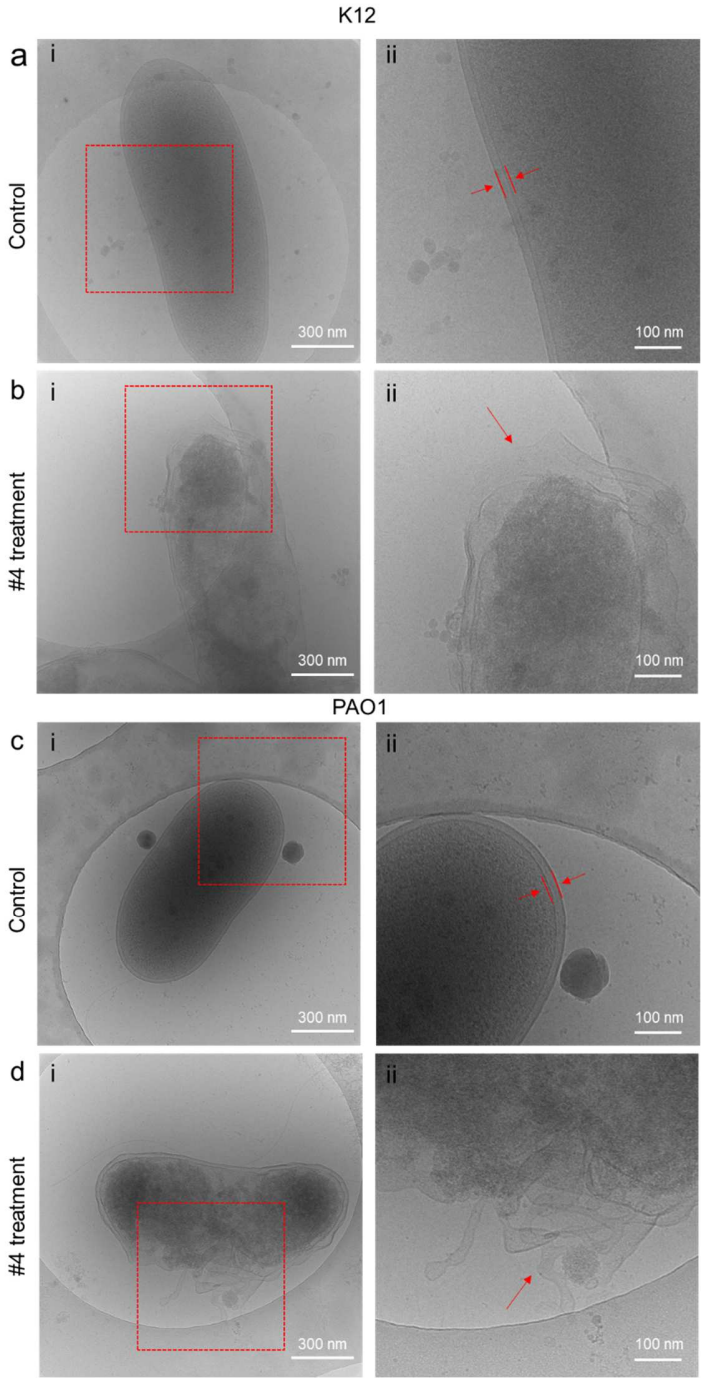

Figure 3. (a)-(d) Cryo-TEM images of untreated *E. coli* K12 (a) and (b) treated with 64 μg/ml of #4. (c)-(d) Cryo-TEM images of untreated *P. aeruginosa* PAO1 (c) and (d) treated with 64 μg/ml of #4. The images shown in the right panels (ii) are enlargements of the indicated areas in the left panels (i). The arrows highlight the membrane lysis.

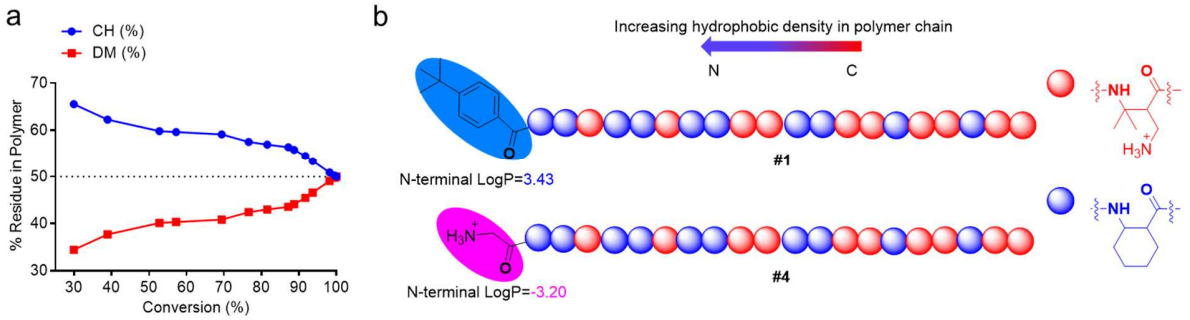

Figure 4. (a) The composition of β-peptide evolution as a function of total monomer conversion. (b) Cartoon representation of the beta-lactam residue sequence. The lipophilicity of the N-terminus (Log P) was calculated from www.molinspiration.com using the blue and pink highlighted atoms in the calculation.

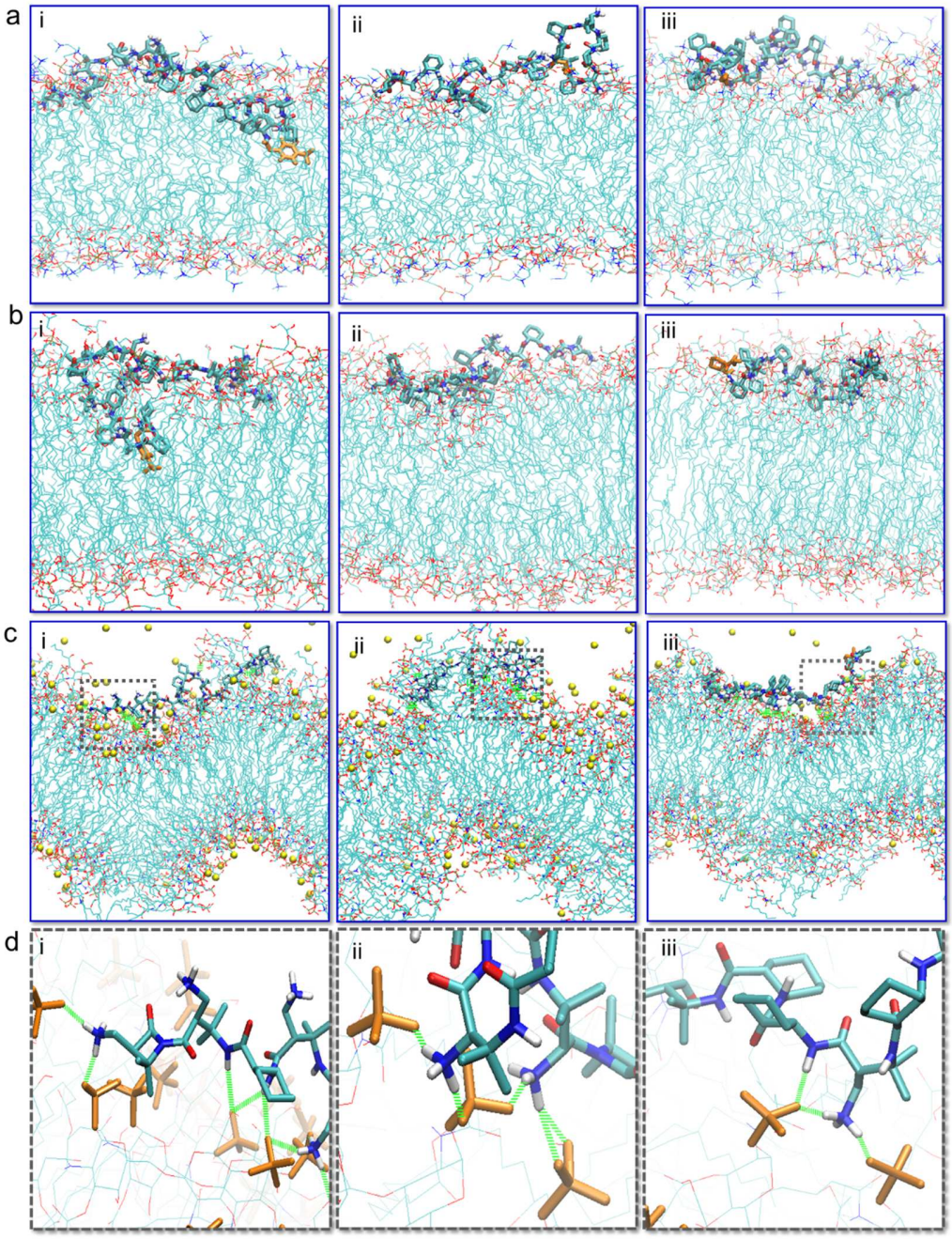

Figure 5. Molecular dynamics simulations of copolymers with model membranes. (a) Snapshots of (i) #1, (ii) #4 and (iii) #5 with mammalian model membrane POPC. Peptides are represented with sticks; the N-terminal residues are in orange. (b) Snapshots of (i) #1, (ii) #4 and (iii) #5 with Gram-positive cytoplasmic model membrane POPG. (c) Snapshots of (i) #1 at 600 ns, (ii) #4 at 420 ns and (iii) #5 at 700 ns with Gram-negative outer membrane lipid A. Individual yellow spheres denote the calcium ions. (d) Enlargements of the indicated areas in (c). The phosphate groups in lipid A are represented with orange sticks. The green dashed lines are the formed hydrogen bonds between the peptide side chain amines and the lipid A phosphate groups.

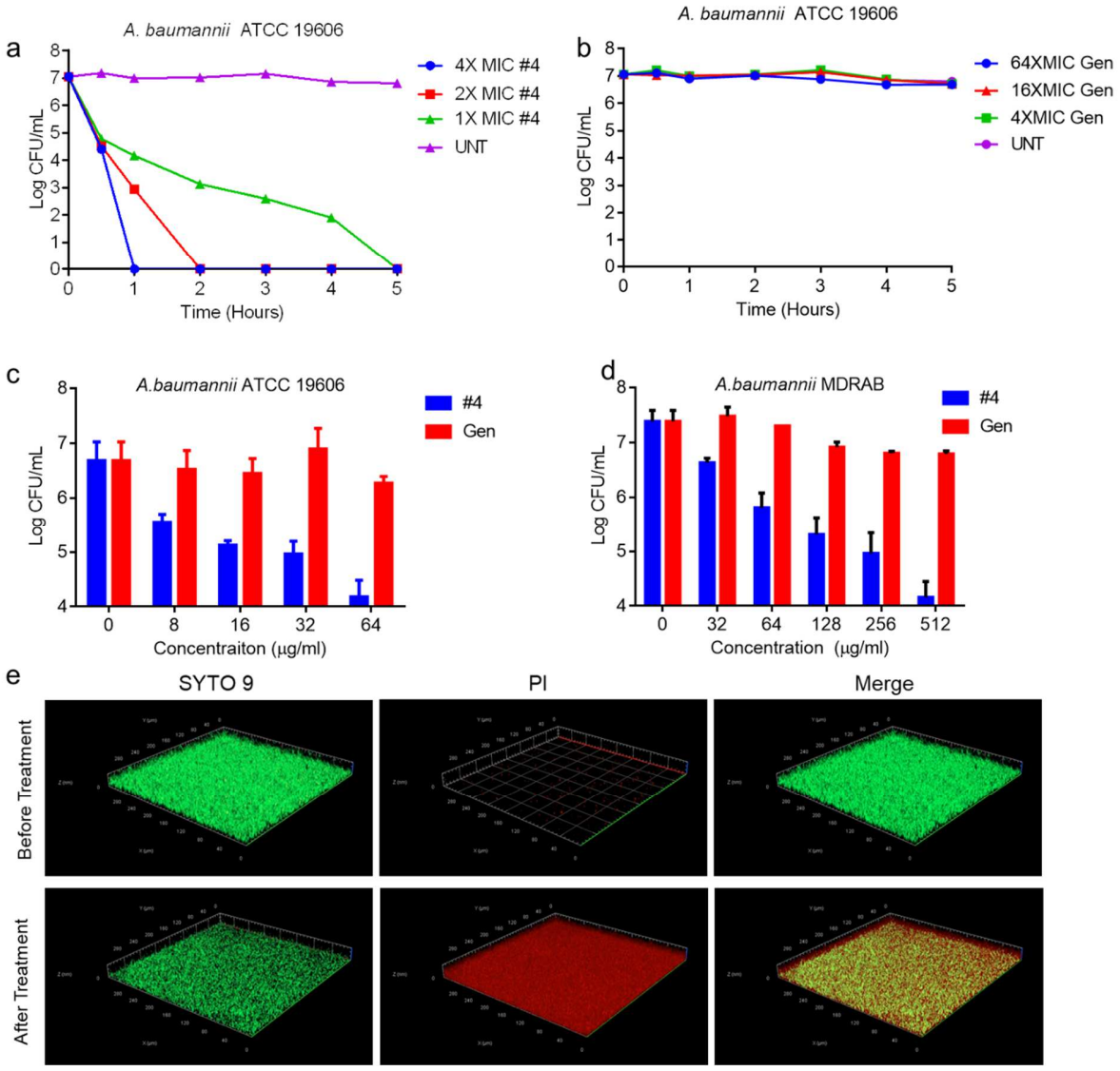

Figure 6. (a) Kill kinetics of #4 against *A. baumannii* ATCC 19606 persisters at 1×, 2× and 4×MIC. (b) Kill kinetics of gentamicin (Gen) against *A. baumannii* ATCC 19606 persisters at 4×, 16× and 64×MIC. (c) #4 and gentamicin efficacy against *A. baumannii* ATCC 19606 in the biofilm environment. (d) #4 and gentamicin efficacy against clinical multi-drug resistant *A. baumannii* MDRAB in the biofilm environment. (e) LIVE/DEAD viability staining of multi-drug resistant *A. baumannii* MDRAB biofilm before and after treatment with #4. Samples were co-stained with SYTO 9 (live, green) and propidium iodide (dead, red) and visualized by confocal microscopy.

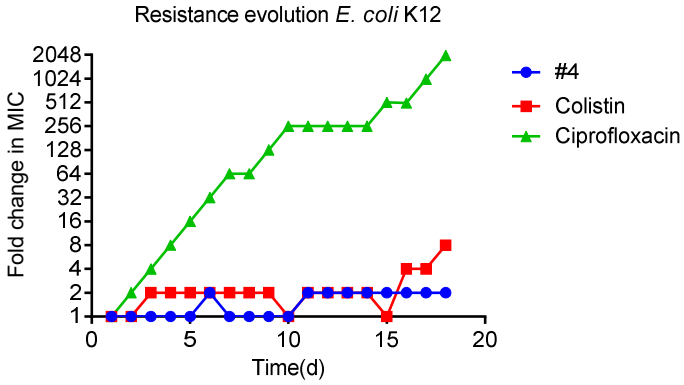

Figure 7. Resistance evolution profile of *E. coli* K12 by serial passages with #4 at sub-MIC. Colistin and ciprofloxacin were used as controls.

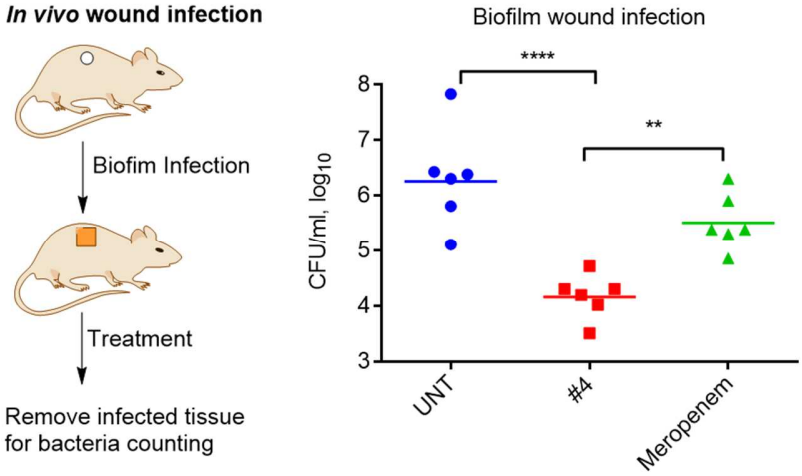

Figure 8. *In vivo* antimicrobial activity of #4 against multi-drug resistant clinical isolate *A. baumannii* MDRAB in a murine biofilm wound infection model. Excision wounds were infected with 5×10^6 CFUs of *A. baumannii* MDRAB and the infection was developed for 24 hours. Mice were subsequently dosed with 3 mg/kg #4, 3 mg/kg meropenem and PBS control (UNT) 3 times at 4 hours intervals. Bacterial counts in the wound site were determined by plating on LB agar plates. Symbols represent the bacterial counts in mice, and the central lines represent the geometric mean of the individual counts (n=6). Statistical analysis was done by one-way ANOVA followed by Dunnett test. P <0.0001 (****); P=0.0062 (**).

Table 1. Summary of antimicrobial activities and biocompatibility of #1-#8.

Entry	MIC (μg/ml)[a]					Cytotoxicity[b] (μg/ml)	Hemolysis[c] (μg/ml)	Selective index[d]	
	Gram-negative			Gram-positive					
	E. coli	*P. aeruginosa*	*A. baumannii*	*S. aureus*	MRSA	IC_{50}	HC_{50}	IC_{50}/MIC	HC_{50}/MIC
#1	16	16	16	16	16	125	312.5	7.81	19.53
#2	32	32	32	32	64	250	625	7.81	19.53
#3	32	32	16	128	128	500	5000	15.62	156.2
#4	16	16	16	64	128	500	5000	31.25	312.5
#5	16	16	16	64	128	500	5000	31.25	312.5
#6	16	16	16	64	128	250	2500	15.62	156.2
#7	16	16	16	32	64	250	312.5	15.62	19.53
#8	32	16	32	32	32	125	156	3.91	4.88

[a]Strains used were: *E.coli* 8739, *P. aeruginosa* PAO1, *A. baumannii* ATCC 19606, *S. aureus* ATCC 29213 and *S. aureus* MRSA BAA40. [b]Cell line used was HEK293. [c]The blood was purchased from InVivos, Singapore. [d]Selective index was calculated against *E. coli* 8739.

Table 2. Antimicrobial activity of #1 and #4 against various Gram-negative and Gram-positive bacteria.

Strains	MICs (μg/ml)	
	#1	#4
Gram-negative		
E. coli 8739	16	16
E. coli K12	8	8
E. coli UT189	16	32
E. coli ATCC 25922	32	16
E.coli ATCC BAA 2774 (CRE)	16	16
P. aeruginosa PAO1	16	16
P. aeruginosa PAW238	4	4
P. aeruginosa PAES	16	16
P. aeruginosa PAD1 (MDR)	16	16
P. aeruginosa PAD25 (MDR)	16	16
P. aeruginosa PAER (MDR)	8	8
P. aeruginosa ATCC 27853	32	16
P. aeruginosa ATCC BAA2797 (MDR)	8	8
A. baumannii ATCC 19606	16	16
A. baumannii ATCC 17978	16	16
A. baumannii ATCC BAA 2803 (MDR)	16	8
A. baumannii ACBAS	8	16
A. baumannii MDRAB (MDR)	16	16
Gram-positive		
S. aureus ATCC 29213	16	64
S. aureus MRSA BAA40 (MDR)	16	128
E. faecium V583 (VRE)	32	128
S. aureus Lac	16	64
S. aureus MRSA USA300	16	64
E. faecium ATCC 29212	32	64
Bacillus cereus ATCC 11778	32	64
Bacillus subtilis ATCC 6633	16	128
S. epidermidis ATCC 700563	16	64
S. epidermidis ATCC 12228	16	64

Table 3. Thermodynamic parameters for #1 and #4 with the model membranes.

Thermodynamic parameters	#1			#4		
	Mammalian membrane[a]	Gram-positive membrane[b]	Gram-negative LPS[c]	Mammalian membrane[a]	Gram-positive membrane[b]	Gram-negative LPS[c]
$K_A(M^{-1})$	16694	21459	26954	NA[d]	5076	29325
ΔG (kJ/mol)	-25.1	-25.7	-26.3	NA[d]	-22.0	-26.5
ΔH (kJ/mol)	1.04	3.68	-50.2	NA[d]	3.47	-48.6
ΔS (J/mol/K)	84.2	94.7	-77.4	NA[d]	82.1	-70.7

[a]Zwitterionic POPC liposome was used to mimic the mammalian plasma membrane; [b]negative charged POPG liposome was used to mimic Gram-positive cytoplasmic membrane; [c]LPS was used to represent Gram-negative bacterial outer membrane. [d]NA means not available due to no interaction.